Proceedings of the 21st ICSMGE, Vienna, Austria, 14 – 19 June 2026. Pistrol, Adam & Schweiger (eds.)
Published by: ÖGG, Austrian Society for Geomechanics, Salzburg, Austria, ISBN 978-3-9503898-4-5
https://doi.org/10.53243/ICSMGE2026-1693

Finite element analysis of the interactions of a high-rise building foundation erected nearby a tunnel with a masonry vault based on monitoring data assimilation

François Boureau, David Arribe
Sixense Engineering, France, francois.boureau@sixense-group.com

David Remaud
Itech-soft SAS, France

ABSTRACT: This article presents a case study of a high-rise building erected in an urbanised area. The vicinity of existing surrounding structures made it necessary to check and control the interactions of the numerous stages of construction of the foundations of the new building (including anchored diaphragm walls). A detailed and comprehensive Finite Element model using the software CESAR-LCPC was used to evaluate the influence of the many parameters of the project. The main objective is to present the wide range of possibilities offered by FEM to investigate numerous aspects of the project. Firstly, specific attention is paid to the reproduction of a realistic stress state in the soil layers. It integrates the history of construction of a sewage collector, a Berlin wall overhanging the diaphragm wall, an unreinforced concrete raft and a tunnel composed of a masonry vault. The latter was extensively studied as on-site instrumentation revealed significant movements. These displacements would be due to swelling or movement of the surrounding soil. Therefore, relevant constitutive models are used for the soils and the structures: an orthotropic and heterogeneous swelling model for the soil surrounding the tunnel; homogeneous anisotropic elasticity associated with a damage model for the masonry vault. In addition, an iterative calibration study (using Python scripts to perform parametric studies with CESAR) made it possible to determine the swelling ratios allowing to reproduce the measured displacements and therefore to assess the present state of conservation of the structure. Given the very strong non-linearities of the model, the iterations are based on the slow but robust Morris method called "one at a time". Finally, the Finite Element results are discussed. They were used to evaluate as accurately as possible the impact of the construction on the tunnel.

KEYWORDS: deep excavation, data assimilation, finite elements analysis, masonry, constitutive models.

1 INTRODUCTION

In today's rapidly densifying urban environments, the imperative to build vertically has become paramount. High-rise developments optimize scarce land resources by accommodating residential, commercial, and mixed-use functions within compact footprints, thereby meeting surging demands for space and economic activity. Yet this upward expansion frequently overlaps with legacy infrastructure—most critically, underground transit systems such as century-old metro tunnels and station caverns. Preserving the integrity and serviceability of these buried assets is essential: even slight ground movements or stress redistributions induced by deep excavations and piling can undermine structural performance, compromise safety, and disrupt urban mobility.

To safeguard sensitive and often antiquated subterranean works, comprehensive instrumentation strategies are indispensable. Deployment of inclinometers, extensometers, vibration sensors, and automated data-acquisition networks enables real-time monitoring of deformation, stress changes, and dynamic responses. Such monitoring not only validates design assumptions but also provides early warning of adverse effects, allowing engineers to implement timely mitigations.

Within this context, the finite element method (FEM) stands out as a powerful decision-support tool. By discretizing soil-structure systems into detailed meshes, FEM facilitates rigorous simulation of soil-structure interaction under various construction scenarios. Coupled with field instrumentation data, finite element models inform parameter calibration, foundation design optimization, and selection of ground-improvement techniques.

Nevertheless, despite these major technical advances, reconciling the results of complex modelling with in situ measurements remains a daunting challenge. This article describes the methodology that made such an endeavour successful.

2 CONTEXT OF THE PROJECT

Our study concerned the construction project of a high-rise building near Paris in an urban environment. A high-rise building exerts high loads on its foundations and the surrounding soil mass. Therefore, to anticipate and quantify this impact, a detailed and comprehensive Finite Element model was performed, and on the other hand, instrumentation was installed on the construction site including surrounding buildings. Especially, a tunnel located just nearby was closely monitored.

During the excavation work, significant displacements were measured in the tunnel. They were probably caused by swelling of the surrounding soil, triggered by unexpected clay hydration phenomena. These movements caused visible damage to the structure. From then on, the challenge was to accurately reproduce these displacements in the FE model.

On-site instrumentation of the tunnel was composed of sets of four topographic targets located in the middle of the vault, on the side walls and in the middle of the raft. These sets were spaced 7,5 meters apart all along the construction site.

3 THE FINITE ELEMENT MODELLING

3.1 *Geometry and meshing*

The typology of the observed damage (longitudinal cracks, bulging distributed in the longitudinal direction) reveals an alteration in the transverse mechanical functioning of the tunnel. This can be modelled in a 2D plane strain finite element model. Furthermore, the plane strain modelling neglects the diffusion of the effects of clay swelling in the longitudinal direction and, in this respect, places us on the safe side.

The model is edited with the commercial software CESAR-LCPC. The detailed geometry (Figure 1) is drawn so that it reflects the soil layers and the several excavations. The foundation of the tower is composed of rectangular bored piles

(green) and anchors (deep blue). In order to limit their influence on the displacements, the limits of the model are placed far from the area of interest where high gradients of strains are computed. Thus, the width of the excavation being 35 m and the section of the tunnel gallery being 17 m, the model is extended 120 m from each lateral side and its base is fixed at -40 m.

The mesh (Figure 2) is composed of 2D isoparametric surface elements (28,214 elements; 55,415 nodes) for the soil layers, the tunnel gallery. The various components of the foundation system, including temporary supports, are modelled with 1D bar elements (prestressed anchors, props) or 1D beam elements (retaining walls, rectangular bored piles in green).

For a pertinent modelling of the soil-structure interaction, joint elements are placed along the vertical walls and the extrados of the tunnel gallery; they follow a classic Coulomb's friction law.

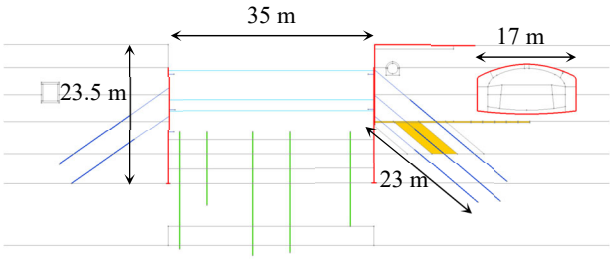

Figure 1. Details of the tower foundation and the tunnel gallery.

3.2 *Constitutive models*

The soil environment of the project is classical in the context of the study area (Figure 3). For the type of structures to be modelled (diaphragm walls), it is generally recommended in France (CFMS 2023) to use an elastoplastic model including hardening for the soil. For this study, we have adopted the widely used Hardening Soil Model (Schanz, 1999) integrated in the catalogue of constitutive models offered by the software CESAR; the required parameters are listed in the Table 1.

The swelling of these soils is modelled as a prescribed strain applied to an area of influence. We can consider two variants: a uniform isotropic strain, or an anisotropic one. In variant 1, the prescribed strain is:

$$\varepsilon_{xx} = \varepsilon_{yy} = \frac{\varepsilon_y}{3} \quad (1)$$

In variant 2, the prescribed strain tensor is anisotropic with:

$$\varepsilon_{xx} = \alpha \cdot \varepsilon_{yy} = \frac{\alpha \cdot \varepsilon_y}{2 \cdot \alpha + 1} \quad (2)$$

All other components are taken as zero.

The material characteristics used for the tunnel vault modelling are taken from the works of Moreno-Regan (2017). They correspond to a Zucchini-type masonry homogenization model coupled with a Mazars damage model (1986) (0). These characteristics were determined from samples taken from Paris Metro tunnels.

The raft slab and the tunnel sidewalls consist of plain concrete. The selected constitutive model is that of an isotropic elastic material incorporating damage, based on the Mazars formulation (1986) (0).

3.3 *Initial stress field and constructions stages*

The objective of the analysis being the modelling of interactions of the foundations works on the tunnel gallery, it is of major importance to start from an accurate initial stress field.

The tunnel has been constructed in the early 19th century. The archives are not accurate enough to the sequence of works. Nevertheless, literature (Moreno-Regan, 2017) and analysis of the existing structure helped to establish a pertinent sequence of construction. The construction of the tunnel is also controlled using the convergence-confinement method (AFTES, 2002), introducing a confinement loss parameter λ that ranges from 0 (perfect confinement) to 1 (no confinement).

Thus, the main points of the construction stages are:

- Initialisation of the geostatic stresses
- Construction of the pile wall
- Tunnel construction:
  - Excavation of the top heading
  - Construction of the masonry vault
  - Excavation of the bench
  - Construction of the side walls
  - Construction of the raft
- Construction of the diaphragm walls
- Excavation to 33.7 m
- 1st line of anchors
- Excavation to 30 m
- 2nd line of anchors
- Excavation to 26.45 m
- 3rd line of anchors
- Volumetric orthotropic expansion of specific soil areas to model the soil swelling
- Various props

3.4 *Contribution of the python scripting*

The data assimilation algorithm requires the finite element models reproducing as faithfully as possible the actual behaviour of the structure and the surrounding soil; above all, it must also include a control script coupled with the modelling software. This later will:

1. Launch the calculation for a given set of parameters
2. Retrieve the modelling results
3. Determine the set of parameters to retain for the next calculation and return to step 1 until the convergence criterion is met

The software CESAR-LCPC offers such possibility. A Python script was written. It helped to control the edition of several components of the model, and it read the results for their efficient extraction and interpretation.

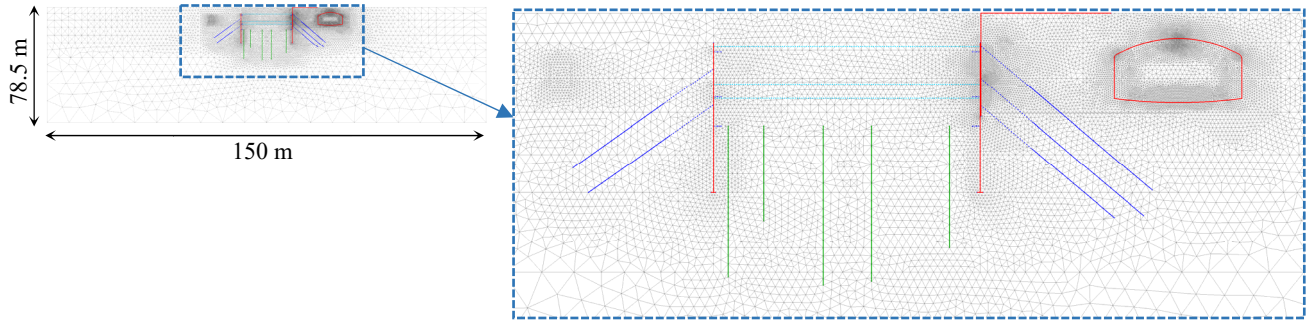

Figure 2. View of the finite element mesh edited in CESAR 2D.

Table 1. Material parameters of the soil layers.

Parameter			Backfill	Old Alluvium	Plastic Clays	Marls	Chalk 1	Chalk 2	Chalk 3
Roof height of the layer		(m)	38.5	30.0	25.5	20.0	15.0	4.5	-5.0
	K_0	(-)	0.5	0.43	0.91	0.5	0.43	0.43	0.43
Unit density	ρ	(kg/m³)	2,100	2,000	2,100	2,200	1,900	1,950	1,950
Unloading/reloading stiffness	E_{ur}^{ref}	(MN/m²)	75	648	87	324	1,512	2,592	5,616
Tangent stiffness	E_{50}^{ref}	(MN/m²)	25	216	29	108	504	864	1 872
Poisson's ratio	ν	(-)	0.2	0.2	0.2	0.2	0.2	0.2	0.2
Cohesion	c	(kN/m²)	10	6	20	20	50	50	50
Friction angle	φ'	(°)	30	35	15	30	35	35	35
Dilatation angle	ψ	(°)	0	0	0	0	0	0	0
Power for stress-level dependency	m	(-)	0.5	0.5	0.8	0.5	0.5	0.5	0.5
Reference pressure	p_{ref}	(kN/m²)	48.3	136.6	206.9	267.1	344.4	436.7	648.1
Failure ratio	R_f	(-)	0.9	0.9	0.9	0.9	0.9	0.9	0.9

Table 2. Material parameters of the tunnel (homogeneisation and damage).

			Masonry vault		Base slab and sidewalls
Parameter			Mortar	Stone	Concrete
Unit density	ρ	(kg/m³)	2,008	2,058	2,127
Young's modulus	E	(MN/m²)	18,400	40,500	21,900
Poisson's ratio	ν	(-)	0.15	0.32	0.21
Compression strength	f_t	(MN/m²)	25.5	75.3	16.6
Tensile strength	f_c	(MN/m²)	1.0	3.4	0.5
Mode I fracture energy	G_{ft}	(N/m².m)	101.4	120.8	103.7
Damage threshold strain	ε_{D0}	(-)	$5.4.10^{-5}$	$8.5.10^{-5}$	$2.18.10^{-5}$
Shear strength	f_s	(MN/m²)	1.4	4.8	0.9
Mode II fracture energy	G_{fs}	(N/m².m)	236.5		
Parameters of Mazars	A_c	(-)	0.71	1.0	0.93
damage model	B_c	(-)	1,000	445	1,550

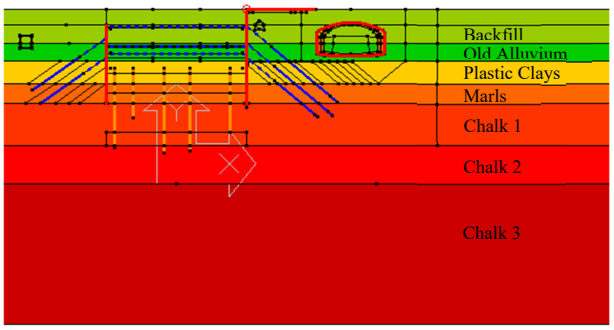

Figure 3. View of soil layers in the modelling

4 CALIBRATION OF THE NUMERICAL MODEL AND ASSESSMENT OF STRUCTURAL SAFETY

4.1 *Parameters*

To model the phenomena that led to the measured displacements in the tunnel, the model includes a load case of orthotropic volume expansion of the soil surrounding the tunnel (see variant 2 of previous chapter 3.2). The soil was divided into independent surface blocks. Each of these blocks undergoes a specific orthotropic volume expansion, determined by two parameters: ε_x, ε_y. Four blocks were distinguished:

- Two blocks in the plastic clays on either side of the tie rod during whose execution swelling phenomena were observed (blocks I and II in yellow on Figure 4)
- Two thin blocks (blocks III and IV in green on Figure 4) located at the roof of the plastic clays, extending from the diaphragm wall to the tunnel. These blocks were added at a later stage because the swelling of the first two blocks was not sufficient to reproduce the measured displacements. These elongated blocks make it possible to reproduce the effects of an extended hydration of the plastic clay layer.

Therefore, 4 x 2 = 8 parameters ε_{xi} and ε_{yi} (with $1 \leq i \leq 4$) to be calibrated so that the theoretical displacements $d_{j,calc}$ obtained match the actual displacements measured $d_{j,obj}$ (with $1 \leq j \leq 10$).

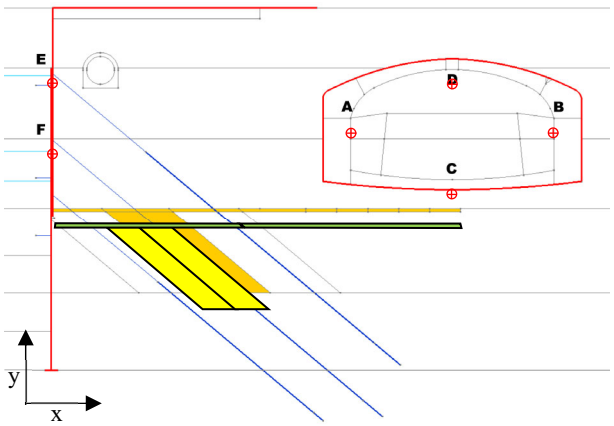

Figure 4. View of the areas subjected to volumetric expansion.

4.2 *Objectives*

Targeted movements are measured movements at the following locations (see also on Figure 4):

- along x and y, 4 specific points A, B, C, D of the tunnel,
- along x, 2 points E and F on the neighbouring diaphragm wall.

Therefore, in total, 10 values are to be respected; they are labelled $d_{i,obj}$, with i=1 to 10.

Usually, the residue R that the algorithm will seek to minimize is the L2 norm of the vector of the differences in displacements between the objective and the calculation results $d_{i,calc}$:

$$R = \sqrt{\sum_i \left(d_{i,obj} - d_{i,calc}\right)^2} \tag{3}$$

Nevertheless, to assess the accuracy of our results, we introduced a second dedicated indicator designed to be less sensitive to measurement noise than the conventional L2 norm. This choice is motivated by the fact that the noise level is only partially proportional to the amplitude of the measured signal, while an irreducible minimum noise level inevitably affects all measurements.

Consequently, the lower the signal amplitude, the more significant the relative impact of noise. To mitigate this effect, we applied a weighting scheme to the squared errors based on the amplitude of the squared target displacement. This formulation yields a residual specifically tailored to capture the accuracy of the solution within the context of a real-world monitoring data assimilation algorithm:

$$R' = \sqrt{\frac{\sum_i {d_{i,obj}}^2 \cdot \left(d_{i,obj} - d_{i,calc}\right)^2}{\sum_i {d_{i,obj}}^2}} \tag{4}$$

It was assumed that convergence may be considered satisfactory for R′<10%.

4.3 *Fitting of the measured displacements with the Morris method*

The model includes very strong nonlinearities in material behaviour, especially damage laws used for the masonry. These nonlinearities invalidate conventional resolution methods such as Newton-Raphson or conjugate gradient. Furthermore, the calculation time for the soil swelling phase (approximately 15 minutes) limits the number of reasonably feasible iterations.

Therefore, we favoured a simpler, slower, and more robust method inspired by the Morris "one at a time" method (1991).

This is used to conduct a sensitivity study of a function around a given point: in an n-dimensional space, the function is evaluated n times by sequentially applying small variations to the parameters of the function. Let f be defined in $\mathbb{R}^n$, with values in $\mathbb{R}$:

$$\boldsymbol{f} : \boldsymbol{X} = (\boldsymbol{x_1}, \ldots, \boldsymbol{x_n}) \rightarrow \boldsymbol{f}(\boldsymbol{X}) \in \mathbb{R} \tag{5}$$

In order to evaluate the sensitivity of f to the different x_i around the point $\boldsymbol{X_0} = (x_{01}, \ldots, x_{0n})$, we evaluate the n values:

$$S_i(\boldsymbol{X_0}) = f(\boldsymbol{X_0} + \boldsymbol{\Delta X_i}) = f(x_{01}, \ldots, x_{0i} + \Delta x, \ldots, x_{0n}) \tag{6}$$

with $\boldsymbol{\Delta X_i}$ being the vector $(\Delta x \times \delta_{ij})_j$

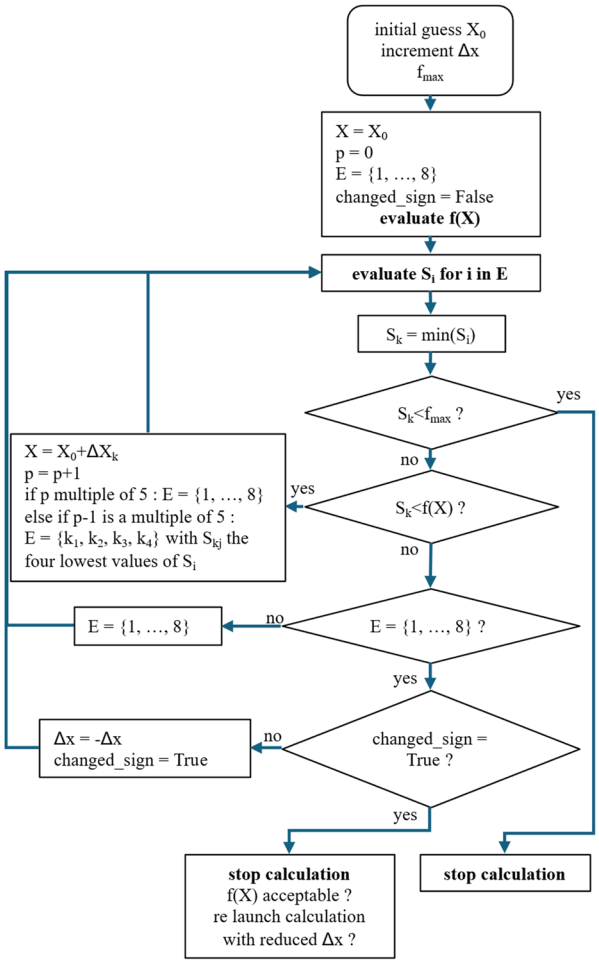

Figure 5. Synoptic diagram of the algorithm for the fitting procedure.

In our case, the function f retained is the residue R' and the parameters x_i are the volume expansion ratios of the soil blocks: at each iteration, the residue is calculated by applying a small variation to the 8 parameters around the current parameter set, the parameter set obtaining the minimal residue is kept and becomes the current parameter set.

The approximate duration of an iteration is therefore 2 hours (8 time 15'). In order to reduce this duration, we decided to calculate the eight values of $S_i(\boldsymbol{X_0})$ only every 5 iterations (complete iteration). During the following 4 iterations, we evaluate the residue for the four indices i producing the minimal residues during the previous complete iteration (partial iteration).

If the residuals obtained are greater than the current residual, the following actions are taken:

1. If the current iteration is partial, a full iteration is performed.

2. If the current iteration is complete, a full iteration is performed by changing the sign of Δx.
3. If, after 1. and 2., the residuals obtained are in all cases greater than the current residual, the algorithm is stopped.

The user must then evaluate the opportunity to restart the algorithm at the point where it stopped by reducing the increment Δx. See Figure 5 for details.

5 RESULTS

The maximum difference obtained between measured and calculated displacements is 18 % (for the most significant displacements). The residues R and R' we obtained are respectively 10.1 mm and 8.7 %. Convergence was regarded as satisfactory (see Figure 6). The calculation lasted for about 12 hours.

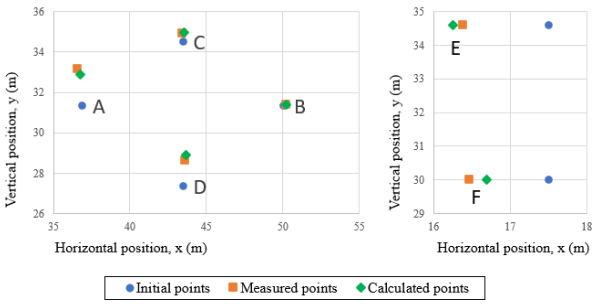

Figure 6. Synthesis of the displacements (measured and calculated) after the fitting procedure. The displacement values were scaled up by 50 to enhance the clarity of the plot.

Since the calculated displacements fitted to measurement, the model was able to provide a realistic mapping of the damage suffered by the tunnel and therefore, to assess its load bearing capacity.

Material degradation is represented by a dimensionless scalar damage variable D for isotropic behaviour and by a damage tensor D_{ij} for orthotropic behaviour (Figure 7). This variable decreases the elastic modulus, accounting for stiffness reduction associated with crack formation and enabling stress redistribution In the specific orthotropic constitutive model we used for the masonry, D11 can be seen as the degradation of the bricks modulus Eb and D22 as degradation of (horizontal) joints modulus Eh. Consequently, this constitutive model offers a more realistic simulation of the material response under severe loading conditions. The damage variables vary from 0 (undamaged) to 1 (fully damaged).

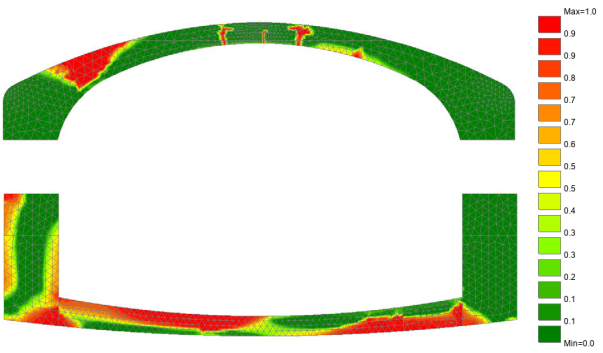

Figure 7. Isoscalar of anisotropic damage indicator D11 in the masonry vault of the tunnel (top) and of isotropic damage indicator D in the plain concrete raft slab and the tunnel sidewalls (down) after volumetric expansion.

Damage-based constitutive laws inherently limit stresses in materials, as they account for the stiffness reduction resulting from local failure. Consequently, the evaluation of the ultimate load of a structure modelled in this way cannot be performed using conventional regulatory criteria for material stress limitation. The procedure adopted to estimate the ultimate load of the structure was as follows:

1. Initial step:
   - application of a uniform nominal surface load F_0;
   - computation of equilibrium for this load F_0;
2. Iterations i: computation of equilibrium for a load i x F_0 until the software fails to find equilibrium;
3. Visualization of the displacements curves $u_{y,i}$ for each iteration i at points A, B, C and D;

The ultimate load is taken as the one corresponding to the onset of a clear divergence in displacement.

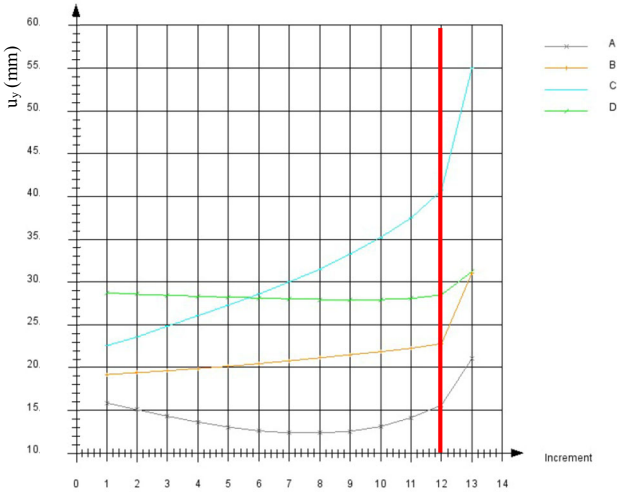

Figure 8. Displacements curves u_y at points A, B, C and D. Failure is obtained at the 12th iteration. F_0=10kPa so the ultimate load is taken as 120kPa

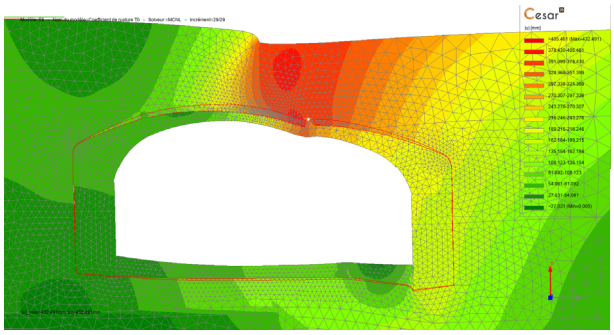

Figure 9. Example of displacements obtained just before failure ($|u|_{max}$ = 432 mm)

6 CONCLUSIONS

The data assimilation algorithm allowed us to reproduce as faithfully as possible the actual damage state of the tunnel and to evaluate in a detailed and optimized manner its level of structural safety. The results also led to adjust the sequence of works of the tower foundations to mitigate their influence on the tunnel structure.

Our study shows how a complex model can be used as a digital twin whose reliability is supported by in-site monitoring and helped engineers and project management decision-making.

7 REFERENCES

AFTES. 2002. La méthode convergence-confinement (GT7R6A1). *Tunnels et Ouvrages Souterrains*, 174, 414-424.

CESAR-LCPC version 2025. FEA software, Reference manual. Available at: https://www.cesar-lcpc.com

CFMS – French ISSMGE Branch. 2023. Recommandations pour la modélisation numérique des ouvrages géotechniques. Technical report.

Mazars, J. A. 1986. Description of micro- and macroscale damage of concrete structures. *Engineering Fracture Mechanics*, 25, 729-737

Moreno Regan, O., Bourgeois E., Colas A.S., Chatellier P., Desbordes A., Douroux J.F. 2017. Application of a coupled homogenization-damage model to masonry tunnel vaults. *Computers and Geotechnics* 83, 132-141. DOI: 10.1016/j.compgeo.2016.10.024

Morris, M. D. 1991. Factorial sampling plans for preliminary computational experiments. *Technometrics* 33(2), 161–174.

Schanz T., Vermeer P.A., Bonnier, B.G. 1999. The hardening soil model: formulation and verification. *Beyond 2000 in Computational Geotechnics*, Balkema, Rotterdam, 281-290.

Zucchini, A. and Lourenço, P.B. 2002. A micro-mechanical model for the homogenisation of masonry, *International Journal of Solids and Structures*, 39, 3233-3255